Cytokine 44 (2008) 221–228

Contents lists available at ScienceDirect

Cytokine

journal homepage: www.elsevier.com/locate/issn/10434666

The distribution of interleukin-19 in healthy and neoplastic tissue ☆

Chung-Hsi Hsing [a,b,h], Hsing-Hui Li [f], Yu-Hsiang Hsu [d], Chung-Liang Ho [e], Shih-Sung Chuang [c,i], Kuo-Mao Lan [a,b], Ming-Shi Chang [a,d,g,*]

[a] Department of Medical Research, Chi-Mei Medical Center, Tainan, Taiwan
[b] Department of Anesthesiology, Chi-Mei Medical Center, Tainan, Taiwan
[c] Department of Pathology, Chi-Mei Medical Center, Tainan, Taiwan
[d] Institute of Biopharmaceutical Sciences, Medical College, National Cheng Kung University, Tainan, Taiwan
[e] Department of Pathology, Medical College, National Cheng Kung University, Tainan, Taiwan
[f] Institute of Basic Medical Science, Medical College, National Cheng Kung University, Tainan, Taiwan
[g] Institute of Biochemistry and Molecular Biology, Medical College, National Cheng Kung University, Tainan, Taiwan
[h] Department of Anesthesiology, Taipei Medical University, Taipei, Taiwan
[i] Department of Pathology, Taipei Medical University, Taipei, Taiwan

ARTICLE INFO

Article history:
Received 21 January 2008
Received in revised form 29 May 2008
Accepted 12 June 2008

Keywords:
Cytokines
Interleukin-19
Tissue microarray

ABSTRACT

The influence of interleukin (IL)-19, a recently discovered cytokine in the IL-10 family, on tissue is still unclear. Our aim was to determine the distribution of IL-19 expression and to delineate the cell types that express IL-19 in healthy and neoplastic tissue, because this information will significantly facilitate the exploration of its pathophysiological functions. We used tissue microarray technology and an immunohistochemical survey with an anti-IL-19 monoclonal antibody to examine the expression of IL-19 in 28 healthy and 15 neoplastic tissues. IL-19 protein was positively stained in 15 healthy tissue types and three major cell types: epithelial cells, endothelial cells, and macrophages. We also found that several types of tumor cells were positively stained for IL-19, especially in squamous cell carcinoma (SCC) of the skin, tongue, esophagus, and lung. SCC of the oral cavity expressed IL-19 mRNA and its receptors. In two cell lines derived from SCC of oral cavity tumor tissue, IL-19 specifically activated an intracellular signal and induced proliferation of the cells, which indicated that IL-19 may act in an autocrine manner in SCC tumors. This study provides important references for further investigation of the biological functions and clinical implications of IL-19 in humans.

1. Introduction

Interleukin (IL)-19, a recently discovered interleukin [1], belongs to the IL-10 family: IL-10, -19, -20, -22, -24 (MDA-7), and -26 (AK155). Despite a partial homology in their amino acid sequences, they are dissimilar in their biological functions [1–5]. At present, only a few biological functions and clinical implications of IL-19 are known. One important cellular source of IL-19 are monocytes, in which lipopolysaccharide (LPS), granulocyte–macrophage colony-stimulating factor (GM-CSF), IL-6, and tumor necrosis factor (TNF)-α upregulate IL-19 expression [6,7]. Although the functions of IL-19 are not well understood, we do know that it induces monocytes to produce IL-6 and TNF-α [8] and CD4-positive (+) T cells to produce Th2 cytokines, which are associated with asthma [9]. IL-19 also induces apoptosis in lung epithelial cells, stimulates liver cells to produce reactive oxygen species (ROS), and promotes neutrophil chemotaxis [10]. Clinically, IL-19 is induced in post-cardiopulmonary bypass inflammatory response and severe sepsis, which indicates that IL-19 may be involved in the pathogenesis of systemic inflammatory diseases [7,10]. Furthermore, IL-19 dose-dependently upregulated IL-4 and downregulated interferon (IFN)-γ [11], which suggested that IL-19 altered the balance of Th1 and Th2 cells in favor of Th2 cells. The expression of IL-19 is also correlated with Th2 cytokine production in patients with uremia [12].

IL-19 has been found in the local tissue of inflammatory lesions. Human psoriatic epidermis tissue samples showed prominent IL-19 immunostaining in their hyperproliferative keratinocytes [13]. In addition, IL-19 upregulated keratinocyte growth factor (KGF) expression in $CD8^+$ T cells [13], which suggested that IL-19 is involved in modulating keratinocyte proliferation. Moreover, the difference in IL-19 expression between healthy and diseased

☆ This work was supported by Grants CMFHR9745 from the Chi-Mei Medical Center and NSC97-2314-B-384-002-MY3 from the National Science Council, Taiwan.

* Corresponding author. Address: Department of Biochemistry and Molecular Biology, National Cheng Kung University, College of Medicine, Tainan 70428, Taiwan. Fax: +886 6 274 1694.
E-mail address: mschang@mail.ncku.edu.tw (M.-S. Chang).

1043-4666/$ - see front matter © 2008 Elsevier Ltd. All rights reserved.
doi:10.1016/j.cyto.2008.06.007

tissue may help to clarify the function of IL-19 in clinical pathophysiology. There are currently no published comprehensive surveys of IL-19 expression in healthy or diseased human tissue or cell types.

A recently developed tissue microarray (TMA) technology—a miniaturized pathology archive for high-throughput in situ studies [14,15]—allows a massive acceleration of correlating molecular in situ findings with clinicopathological information. Sections from TMA blocks can be used for different types of in situ tissue analysis, including immunohistochemistry and in situ hybridization [14–16]. The tissue microarray approach is useful in surveys of tumor populations and can be used to comprehensively analyze the functions of newly identified genes in both healthy and neoplastic human tissue [15–17]. To explore the relation between IL-19 and biological functions in human, we developed monoclonal antibodies against human IL-19. Using TMA and immunohistochemical staining with these antibodies, we surveyed IL-19 expression in healthy and neoplastic human tissues.

2. Materials and methods

2.1. Human tissue microarrays

Commercialized tissue microarrays (TMAs) (Pantomics, Inc, San Francisco, CA) with 28 types of healthy human tissue (Table 1) were used for immunohistochemical staining. The TMAs were designed following the FDA-recommended healthy tissue panel for antibody cross-reactivity testing described in the manufacturer's instructions. Tumor TMAs were obtained from the Pathology Department of the National Cheng Kung University Medical College. Fifteen neoplastic (Table 2) tissue samples, formalin-fixed and paraffin-embedded, were retrieved from the archive. There were three samples of each healthy and neoplastic tissue type, one each from different donors. The TMAs were constructed using a custom-made arrayer described elsewhere [14].

Table 1
Immunostaining of IL-19 in healthy tissue

	Epithelial cells	Endothelial cells	Macrophages[a]	Others
1. Skin	++	+		
2. Lung	+	+	++	
3. Liver	+[b]			
4. Kidney	+[c]	+		
5. Prostate	+[d]			++[e]
6. Pancreas				
7. Adrenal	++[d]			
8. Pituitary				+[f]
9. Thyroid				
10. Parathyroid				
11. Heart		+		
12. Fallopian tube				
13. Esophagus				
14. Stomach				
15. Small intestine			+	
16. Colon			+	
17. Rectum			+	
18. Ovary				
19. Placenta		+		+[g]
20. Spleen			+/−	
21. Skeletal muscle				
22. Testis				+[h]
23. Thymus				
24. Tonsil				
25. Ureter				
26. Uterine cervix	+/−			
27. Uterine endometrium				
28. Brain				

++, strongly stained; +, moderately stained; +/−, weakly stained.
[a] Confirmed using CD68 immunostaining.
[b] Hepatocytes.
[c] Renal tubular cells.
[d] Glandular epithelial cells.
[e] Myoepithelial cells.
[f] Pituitary gland endocrine cells.
[g] Trophoblasts.
[h] Germ cells.

Table 2
Tumor cells stained for IL-19 in neoplastic tissue

Tumor type	IL-19 immunostaining
1. Skin, SCC	+
2. Buccal mucosa, SCC	++
3. Tongue, SCC	++
4. Esophagus, SCC	++
5. Lung, SCC	+
6. Breast, IDC	++
7. Liver, HCC	+
8. Kidney, RCC	+
9. Ovary, clear cell carcinoma	+
10. Bladder, TCC	+/−
11. Thyroid, papillary carcinoma	+/−
12. Thymus, thymic carcinoma	+/−
13. Lymph node, B cell lymphoma	+/−
14. Stomach, adenocarcinoma	−
15. Colon, adenocarcinoma	−

++, strongly stained; +, moderately stained; +/−, weakly stained; −, not stained.
SCC, squamous cell carcinoma; IDC, infiltrating duct carcinoma; HCC, hepatocellular carcinoma; RCC, renal cell carcinoma; TCC, transitional cell carcinoma.

2.2. Malignant tumor samples

Formalin-fixed, paraffin-embedded malignant tumor samples were retrieved from the archive: squamous cell carcinoma (SCC) of the skin, oral cavity, esophagus, and lung; renal cell carcinoma (RCC); infiltrating duct carcinoma (IDC) of the breast; hepatocellular carcinoma (HCC); and adenocarcinoma of stomach and colon. Eight or nine cases of each tumor were retrieved. Whole sections of each tissue block were prepared for the immunohistochemistry study.

2.3. Reverse transcriptase-polymerase chain reaction (RT-PCR)

Human tissue samples obtained from the Tumor and Serum Bank of Chimei Medical Center were used to analyze the transcripts of IL-19 and its receptors, IL-20R1 and IL-20R2. Each type of tissue included three samples from different donors. The total RNA of the selected tissue was extracted using RNA-Bee isolation reagent (Tel-Test Inc., Friendswood, TX). Oligo(dT)21-primed first-strand cDNA was synthesized using reverse transcriptase. We used PCR to amplify IL-19 and its receptors' transcripts from cDNA. The sense primer (5′-gct gcg tga cca aga acc tcc tgg-3′) and antisense primer (5′-tag act ctg gtg gca ttg gt-3′) were used for IL-19. The sense primer (5′-agc tgg aca gcg aag gaa ta-3′) and antisense primer (5′-agt gtg tga cca acc aca cg-3′) were used for IL-20R1. The sense primer (5′-gaa gtg gcc att ctg cct gcc-3′) and antisense primer (5′-ggg aat ggc ctc tcc ttg cac-3′) were used for IL-20R2. PCR products were visualized on 1.5% agarose gels containing ethidium bromide.

2.4. Expressing and purifying IL-19 recombinant protein

A cDNA clone coded for the human IL-19 sequence from leucine to leucine (amino acids 25–176) was inserted into the expression vector of *Pichia pastoris* (pPICZ-α; Invitrogen, San Diego, CA). We used affinity chromatography to express and purify human IL-19 from the culture medium of the yeast cells. This protein was used to generate monoclonal antibodies as described below.

2.5. Generating mouse monoclonal antibodies against human IL-19

Mouse monoclonal antibodies (mAb) against human IL-19 (1BB1) were generated as previously described [9]. Selecting and characterizing mAb against human IL-19 followed the standard protocols [18]. We determined the epitope specificity of a panel of mAb by testing the ability of pairs of mAb to bind simultaneously to the antigen in ELISA. In brief, the capture antibody was attached to a solid substrate; the antigen (IL-19) was then attached to the substrate, and the ability of the biotin-labeled detection antibody to bind with the antigen was monitored.

2.6. Immunohistochemistry

Paraffin-embedded-tissue slides with microarray samples were used for immunohistochemical staining with human IL-19 mAb and anti-CD68 antibody (DakoCytomation, Carpinteria, CA), respectively. The immunostaining of IL-19 was done as previously described [13]. The paraffin on a series of 5-mm sections was removed using xylene. The sections were then rehydrated using a graded ethanol series. The sections were immersed in a 10-mM sodium citrate solution at 93 °C for 20 min to retrieve the antigen; next, the sections were washed with tap water. The slides were then soaked in 90 ml of methanol/10 ml 30% H_2O_2 for 10–15 min at room temperature to block endogenous peroxidases, and then washed with PBS. The slides were blocked by immersing them in antibody diluent with background-reducing components (DakoCytomation) for 10 min to suppress non-specific immunoglobulin staining. They were then incubated with purified mAb (diluted 1:50) against human IL-19 or anti-CD68 antibody (diluted 1:100) in blocking reagent at 4 °C overnight. The pre-absorption test was done before the paraffin tissue sections had been incubated with recombinant IL-19 protein and 1BB1 (ratio, 10:1). Incubating paraffin tissue sections with mouse IgG1 isotype (clone 11711; R&D Systems, Minneapolis, MN) instead of primary antibody was the negative control. The slides were then treated consecutively with HRP-conjugated goat anti-mouse IgG (Biolegend, San Diego, CA) (diluted 1:200) and incubated for 2 h at room temperature. Next, the slides were incubated using an AEC or DAB substrate kit (Vector Laboratories, Burlingame, CA), and the color reaction was allowed to develop for 5–10 min. After the staining reaction, the slides were washed thoroughly in tap water, counterstained with Mayer's hematoxylin (ThermoShandon, Pittsburgh, PA), and mounted with cover slides.

2.7. Real-time PCR analysis of the IL-19 transcript

To amplify the IL-19 transcript, real-time PCR was performed using the LightCycler-Fast Start DNA Master SYBR Green I kit (Roche, Indianapolis, IN) according to the manufacturer's instructions. The sense primer (5′-gct gcg tga cca aga acc tcc tgg-3′) and antisense primer (5′-tag act ctg gtg gca ttg gt-3′) were used in real-time PCR following the standard protocol. Individual PCR products were analyzed using melting-point analysis. β-Actin was used as an internal control gene to normalize for RNA amounts. Real-time PCR product was analyzed using the comparative C_t method according to the manufacturer's instructions. In brief, sample variation was corrected by subtracting β-actin C_t values from the C_t values (=ΔC_t) of the IL-19.

2.8. Western blot analysis

For Western blot analysis, cells (1×10^6) were plated in 60-mm dishes and starved for 24 h before stimulation. The cells were then stimulated with human IL-19 (8 nM) for the indicated time. Western blot analysis was done using antibody specific for phosphor-AKT (Cell Signaling Technology, Inc., Beverly, MA) or α-tubulin (Santa Cruz Biotechnology, Santa Cruz, CA) following the manufacturer's instructions.

2.9. Cell proliferation assay

OEC-M1 and OC3 cells, two cell lines derived from SCC of the oral cavity [19,20] were cultured in growth medium without fetal calf serum for 16 h, and then exposed to various concentrations of IL-19 for 48 h. Cells were then incubated with a 1 mg/ml solution of 3-[4,5-dimethylthiazol-2-yl]-2,5-diphenyltetrazolium bromide (MTT) (Sigma–Aldrich, St. Louis, MO) for 3 h. DMSO (dimethyl sulfoxide) (Sigma) was added to the culture, and absorbance was determined to be 550 nm. Fetal bovine serum (10%) (Sigma) was used as the positive control. To demonstrate the specific activity of human IL-19, monoclonal antibody 1BB1 against human IL-19 at a concentration of 10:1 (1BB1:IL-19) was added alone or together with human IL-19 into cells, and the proliferation of cells was monitored.

2.10. Data analysis

Staining results were read by two pathologists (CLH and SSC) blinded to each other's scoring. The stained TMA slides were visually scored as strongly stained, moderately stained, weakly stained, and not stained. Both pathologists arrived at similar results. Differences of proliferation between groups of cells were evaluated using the Kruskal–Wallis ANOVA test and then Dunn test. Statistical significance was set at $P < 0.05$. Analysis was performed using commercial software (SigmaPlot 9.0; Systat Software Inc., Point Richmond, CA).

3. Results

3.1. IL-19 was expressed in specific tissue types

IL-19 protein was stained in 15 of 28 healthy tissue types (Table 1). Selected immunohistochemical micrographs from the tissue microarrays immunostained with monoclonal antibodies raised against human IL-19 are shown in Fig. 1. The major cell types stained specifically positive for IL-19 were epithelial cells, endothelial cells, and macrophages. Non-specific immunostaining did not occur when the mouse IgG1 isotype was used as the negative control or when a pre-absorption test was done in the immunohistochemical protocol (data not shown). To confirm the expression of IL-19, RNA was extracted and analyzed using RT-PCR in nine non-pathological human tissue samples (Fig. 2). IL-19 transcripts were expressed in heart, lung, spleen, and placenta tissue; these results were consistent with the immunohistochemical staining.

3.2. Epithelial and myoepithelial cells were stained positive for IL-19

Several types of tissue were stained positive for IL-19 in epithelial cells: skin, lung, liver, kidney, prostate, adrenal gland, and uterine cervix tissue (Table 1). In skin tissue, IL-19 was strongly stained in the squamous epithelial cells of the basal epidermis (Fig. 1A) and sweat glands. These IL-19-positive squamous epithelial cells were accentuated in the stratum basale of skin tissue. In contrast, IL-19 was not stained in the squamous epithelial cells of esophagus tissue (Fig. 1B) and only weakly stained in uterine cervix tissue (Table 1). In lung tissue, alveolar epithelial cells were stained for IL-19 (Fig. 1C). In liver tissue, IL-19 was moderately stained in hepatocytes (Fig. 1D). In kidney tissue, renal tubular cells were stained positive for IL-19 (Fig. 1E). In prostate tissue, glandular epithelial

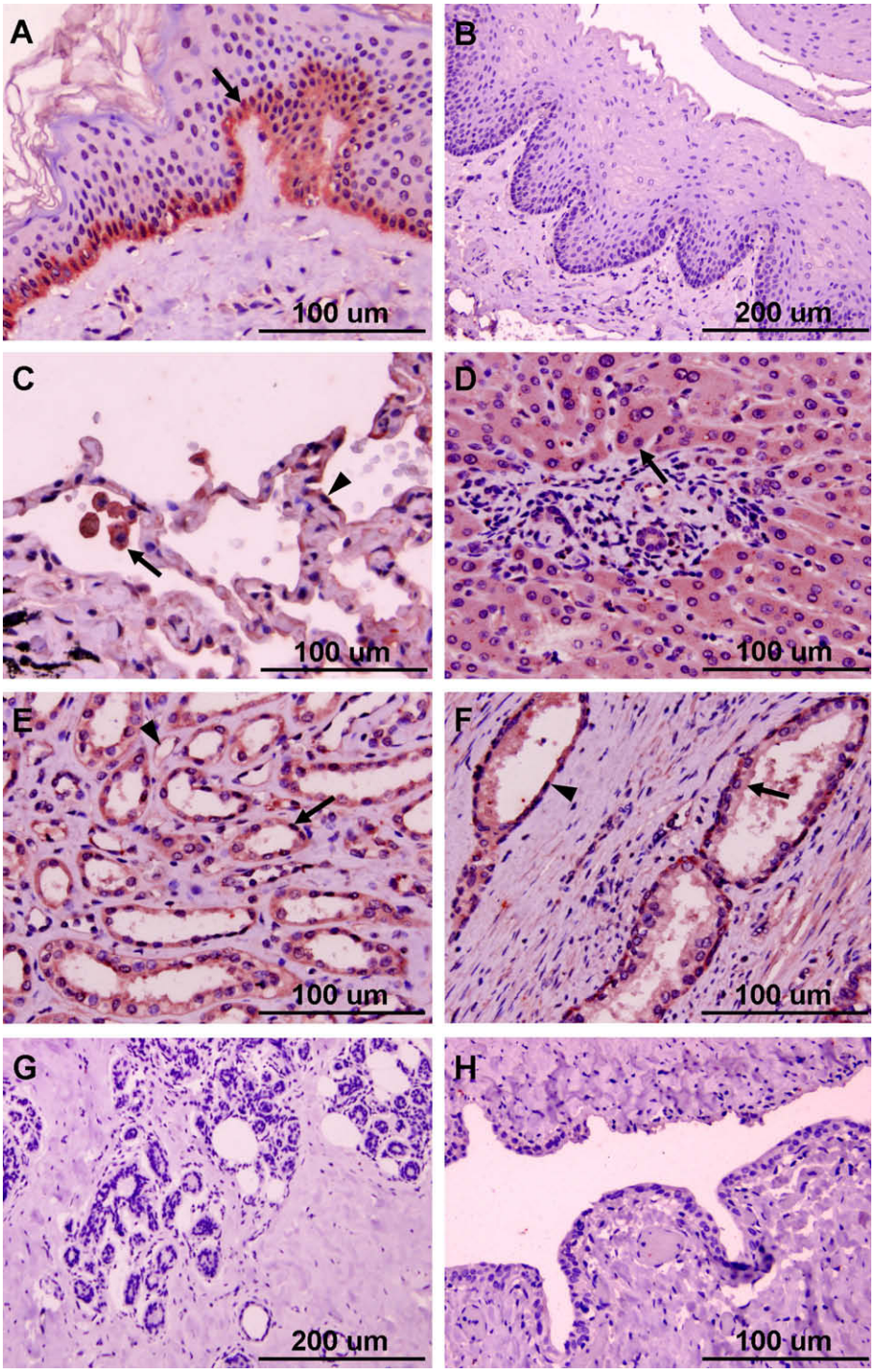

Fig. 1. Immunohistochemical staining of IL-19 in selected healthy human tissue types on the TMA. IL-19 was strongly stained in squamous epithelial cells (arrow) in skin (A) but not in esophagus tissue (B). In lung tissue, IL-19 was strongly stained in macrophages (arrow) and epithelial cells (arrowhead) (C). In liver tissue, IL-19 was moderately stained in hepatocytes (D). In kidney tissue, renal tubular cells (arrow) and capillary endothelial cells (arrowhead) were stained positive for IL-19 (E). In prostate tissue, IL-19 was moderately stained in glandular epithelial cells (arrow) and strongly stained in myoepithelial cells (arrowhead) (F). None of the cells in breast (G) or ureter tissue (H) were positively stained for IL-19.

cells and myoepithelial cells surrounding the prostate glands were stained positive for IL-19 (Fig. 1F). In adrenal gland tissue, glandular epithelial cells were strongly stained for IL-19 (Table 1). The glandular epithelial cells of breast tissue (Fig. 1G) were not stained for IL-19. Most epithelial cells in gastrointestinal and urinary tract tissue were not stained for IL-19 (Table 1 and Fig. 1H).

3.3. Endothelial cells were stained positive for IL-19

The endothelial cells of small vessels in skin, lung, kidney, heart, and placenta tissue were stained positive for IL-19 (Table 1). In kidney tissue, anti-IL-19 antibody highlighted most of the capillary endothelial cells between the renal tubules (Fig. 1E, arrowhead).

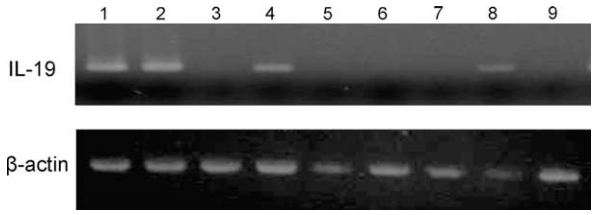

Fig. 2. IL-19 transcripts were expressed in non-pathological tissue. Total RNA extracted from non-pathological human tissue and IL-19 transcripts were amplified using RT-PCR. 1: heart, 2: lung, 3: pancreas, 4: spleen, 5: thyroid, 6: skeletal muscle, 7: stomach, 8: placenta, 9: ureter. β-Actin was an internal control. Similar results were found in tissue samples from three different donors.

3.4. Macrophages were stained positive for IL-19

We found IL-19 protein in macrophages in lung (Fig. 1C), small intestine, colon, rectum, and spleen tissue (Table 1). To colocalize IL-19 with CD68 positive cells, we used separate stainings for IL-19 and CD68 from neighboring sections on the same tissue slide. These macrophages were stained positive for CD68 (data not shown).

3.5. Tumor cells in different neoplastic tissue samples were stained positive for IL-19

Tumor cells in 13 of 15 neoplastic tissue samples were stained positive for IL-19 at various levels (Table 2). In tissue from SCC of the tongue (Fig. 3A) and esophagus (Fig. 3B), most tumor cells were strongly stained for IL-19. Infiltrating duct carcinoma (IDC) of the breast tumor cells showed strongly positive immunostaining (Fig. 3C). Hepatocellular carcinoma (HCC) (Fig. 3D), renal cell carcinoma (RCC) (Fig. 3E), and clear cell carcinoma of the ovary tumor cells were moderately stained for IL-19. Transitional cell carcinoma (TCC) tumor cells of the bladder, thymic carcinoma, and lymphoma were weakly stained for IL-19 (Table 2). However, most adenocarcinoma (AC) of the stomach and colon (Fig. 3F) tumor cells were not stained for IL-19. To further determine if immunostaining indeed reflected IL-19 gene expression in the neoplastic tissues, we performed real-time PCR analysis on the neoplastic tissues with different levels of immunostaining. SCC of oral cavity and IDC of breast (strongly stained), SCC of lung (moderately stained), TCC of bladder (weakly stained), and AC of colon (non-stained) were analyzed for IL-19 transcripts ($n = 3$ in each tumor). AC of colon

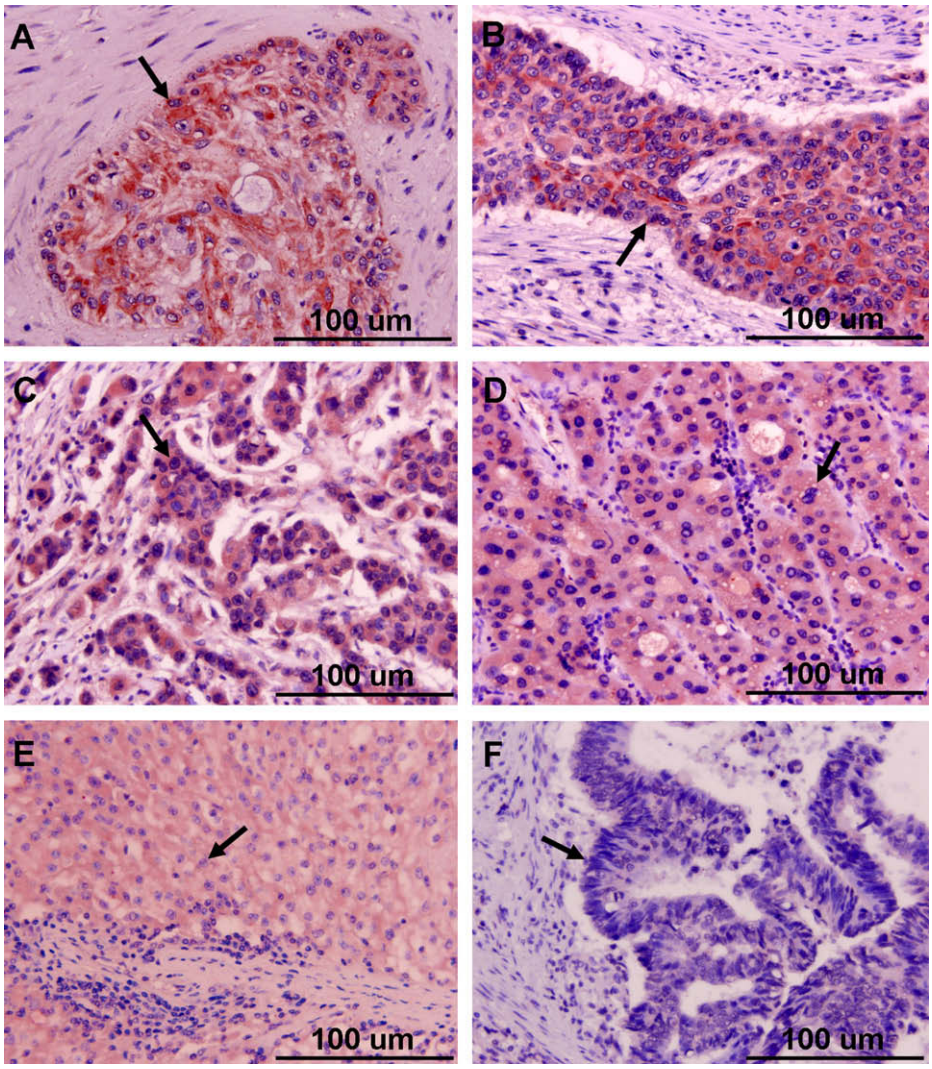

Fig. 3. Different types of tumor cells expressed various patterns of IL-19 in neoplastic tissue. In squamous cell carcinoma of the tongue (A) and esophagus (B), most tumor cells (arrows) were strongly stained for IL-19. Tumor cells in infiltrating duct carcinoma (IDC) of the breast (C) showed strongly positive IL-19 immunostaining (arrow). Tumor cells in hepatocellular carcinoma of the liver (D) and renal cell carcinoma of the kidney (E) were moderately stained for IL-19 (arrows). In adenocarcinoma of the colon (F), the tumor cells (arrow) were not stained for IL-19.

tissues expressed the least levels of IL-19 transcripts than other tumor tissues. In comparison with AC of colon tissues, the SCC of oral cavity, IDC of breast, SCC of lung, and TCC of bladder tissues expressed higher levels of IL-19 transcripts (5.2-, 4.7-, 5.0-, and 2.8-fold, respectively) (Fig. 4).

3.6. A high percentage of carcinoma cells were stained positive for IL-19

Many carcinoma tissue samples in the TMA were positively stained for IL-19. To determine whether IL-19 was indeed stained in the whole section of carcinoma tissue, we stained, with anti-IL-19 mAb, archived tissue samples from 34 cases of SCC, 8 cases of RCC, 9 cases of IDC, 9 cases of HCC, and 18 cases of adenocarcinoma. A high percentage of SCC, RCC, IDC, and HCC samples, but not adenocarcinoma samples, showed strong-to-moderate positive IL-19 immunostaining (Table 3).

3.7. IL-19 activated intracellular signal in oral cancer cell lines

Many SCC tissue samples were strongly stained for IL-19. RT-PCR analysis of 3 SCC tumor samples of the oral cavity also showed mRNA expression of both IL-19 and its receptors, IL-20R1 and IL-20R2, in all three samples (Fig. 5). We hypothesized that IL-19 may act on tumor cells in an autocrine manner. Thus, we chose oral cancer cell lines as a model to study the effect of IL-19 on oral cancer cells. OEC-M1 and OC3 cells expressed the mRNA of both IL-19 and its receptors IL-20R1/IL-20R2 (data not shown). We treated OEC-M1 and OC3 cells with IL-19 and analyzed the effect of IL-19 on intracellular signaling. After the cells were treated with IL-19, the intracellular AKT signal was activated (Fig. 6 A and B), while ERK and p38 were not significantly activated (data not shown). The

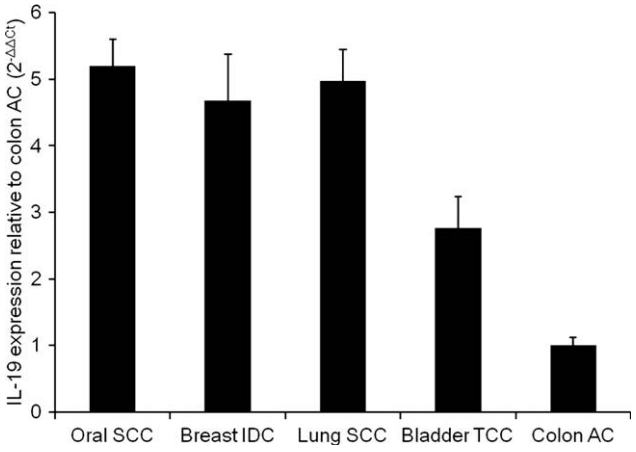

Fig. 4. IL-19 transcripts in neoplastic tissues. Transcripts of IL-19 in SCC of oral cavity, IDC of breast, SCC of lung, TCC of bladder, and AC of colon were determined using reverse transcription-quantitative real-time PCR. Three patient samples for each tumor were analyzed. β-Actin was an internal control. Values are expressed as $2^{-\Delta\Delta C_t}$, relative to the levels of AC of colon and corrected using β-actin expression. Data are means ± SEM. SCC, squamous cell carcinoma; IDC, infiltrating duct carcinoma; TCC, transitional cell carcinoma; AC, adenocarcinoma.

Table 3
Percentage of tumors stained positive for IL-19

	n	IL-19 immunostaining			
		Strong *n* (%)	Moderate *n* (%)	Weak *n* (%)	None *n* (%)
Squamous cell carcinoma					
Skin	8	2 (25)	5 (62)	1(12)	0 (0)
Oral cavity	9	5 (55)	4 (44)	0 (0)	0 (0)
Esophagus	8	4 (50)	3 (37)	1 (12)	0 (0)
Lung	9	2 (22)	5 (55)	2 (22)	0 (0)
Kidney, RCC	8	0 (0)	4 (50)	4 (50)	0 (0)
Breast, IDC	9	2 (22)	7 (77)	0 (0)	0 (0)
Liver, HCC	9	1 (11)	6 (66)	2 (22)	0 (0)
Adenocarcinoma					
Stomach	9	0 (0)	0 (0)	1 (11)	8 (88)
Colon	9	0 (0)	0 (0)	1 (11)	8 (88)

IDC, infiltrating duct carcinoma; RCC, renal cell carcinoma; HCC, hepatocellular carcinoma.

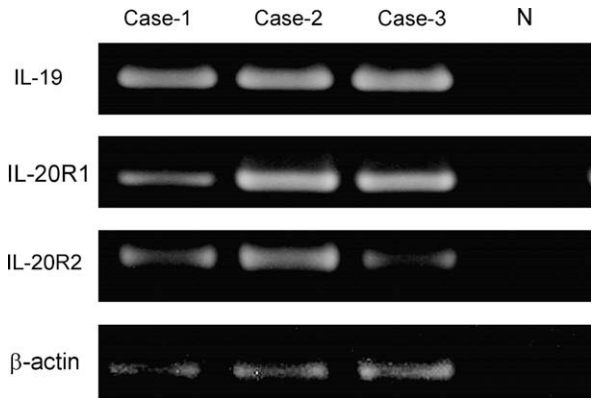

Fig. 5. Transcripts of IL-19 and its receptors IL-20R1/IL-20R2 in three tissue samples of SCC of the oral cavity (case-1, case-2, and case-3) were amplified using RT-PCR.

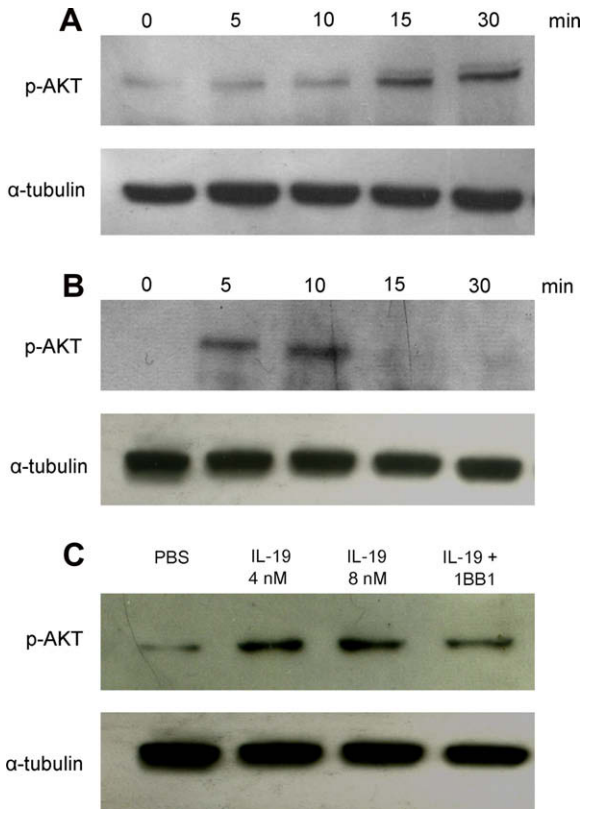

Fig. 6. IL-19 activated intracellular signals in oral cancer cell lines. We analyzed, using Western blotting, the intracellular AKT signal of OEC-M1 (A) and OC3 (B) cells after they were treated with IL-19 (8 nM) at the indicated times. (C) IL-19 (4 and 8 nM/ml) activated AKT signal in OEC-M1 cells after 30 min treatment, which was attenuated by anti-IL-19 monoclonal antibodies (1BB1, 20 nM). Similar results were obtained in three independent experiments.

phospho-AKT in OEC-M1 cells was activated by IL-19 and attenuated by anti-IL-19 monoclonal antibodies (Fig. 6C) which indicated that the activity of IL-19 on OEC-M1 cells is specific.

3.8. IL-19 induced proliferation of oral cancer cell lines

We next determined the effect of IL-19 on proliferation of oral cancer cell lines. We treated OEC-M1 cells with IL-19 (2, 4, and 8 nM) for 48 h and determined the cells proliferation using MTT assay. IL-19 induced proliferation of OEC-M1 cells (Fig. 7A) in a dose-dependent manner. In addition, IL-19 (8 nM) also induced proliferation of OC3 cells (Fig. 7B). These proliferation responses were attenuated by anti-IL-19 monoclonal antibodies (Fig. 7 A and B).

4. Discussion

Knowledge about the influence of IL-19 on tissue is still incomplete. So far, IL-19 has been found in LPS-treated monocytes, skin keratinocytes, and bronchial epithelial cells [6,21–24]. Further exploring the expression and distribution of IL-19 in all tissues and cell types may help us to investigate the impact of IL-19 in the pathophysiology of human diseases.

In the present study, using a tissue microarray and immunohistochemical staining, we presented a survey of the distribution of IL-19 protein in 28 types of healthy human tissue and 15 types of neoplastic tissue. We found that 15 of 28 types of healthy tissue were stained positive for IL-19. We also verified the TMA results with a semi-quantitative analysis and clarified the IL-19-positive-staining cell types in healthy tissue. The major cell types that stained positive for IL-19 were epithelial cells, endothelial cells, and macrophages the finding was not previously reported. In addition, we also showed that 13 of 15 malignant tumor cells, especially SCC, RCC, IDC, and HCC, were stained positive for IL-19.

We previously reported [25] the tissue distribution of IL-20 using TMAs. Both IL-19 and IL-20 were stained in the cell types: epithelial cells, myoepithelial cells, endothelial cells, and macrophages. However, they are expressed in different tissue types. Epithelial cells in liver, kidney, and uterine cervix tissue were positively stained for IL-19 but not for IL-20. In contrast, epithelial cells in breast, fallopian tube, and ureter tissue were positively stained for IL-20 but not for IL-19. Tissue macrophages stained for IL-19 were less widely distributed than those stained for IL-20. Skeletal muscle cells were stained positive for IL-20 [25] but not for IL-19, which was consistent with the mRNA expression confirmed using RT-PCR (Fig. 2).

IL-19 shares a receptor complex with IL-20, indicating that some of the biological activities of these two cytokines might overlap. For example, both IL-19 and IL-20 were strongly stained in skin epidermis and induced KGF production in $CD8^+$ T cells, which suggested that both cytokines might be involved in keratinocyte proliferation [13,26] and skin diseases. However, the disparate expression of these two cytokines in the tissues suggests they also have dissimilar biological roles.

It is interesting that most of malignant tumors in this study were positively stained for IL-19. We found that all of SCC of the skin, oral cavity, esophagus, and lung were stained positive for IL-19, but adenocarcinoma tissue from the gastrointestinal tract was not. Notably, squamous epithelial cells of healthy esophagus were not stained positive for IL-19, while tumor cells of SCC of esophagus were strongly stained for IL-19. We also demonstrated that the intensity of IL-19 immunostaining was correlated with the transcript level of IL-19 in SCC of oral cavity, IDC of breast, TCC of bladder, and AC of colon. However, tumor cells of SCC of lung were moderately stained for IL-19, while their IL-19 transcript was shown to be as high as those of SCC of oral cavity and IDC of breast tissues. The discrepancy may be due to the variation between patients or different stages of lung cancer. Further investigation will be required to explore if IL-19 expression level correlates with progression of lung cancer. In our previous report [13], immunostaining of IL-19 on psoriasis tissue showed upregulation of IL-19 in psoriasis patients. IL-19 may upregulate KGF production and be involved in modulating keratinocyte proliferation and the pathogenesis of psoriasis [13]. In this study, IL-19 was strongly stained in SCC of buccal mucosa, tongue, and esophagus with the staining intensity similar to that of psoriasis (data not shown). Moreover, IL-19 induced intracellular AKT phosphorylation and cell proliferation in oral cancer cell lines. Thus, IL-19 might play an important role in the pathogenesis of SCC.

We also found that healthy breast tissue was not positively stained for IL-19, but breast IDC tissue was strongly stained for IL-19. This finding is compatible with a previous report [27] of abundant IL-19 mRNA expression in breast-cancer cell lines. Thus, the detailed mechanism how IL-19 is involved in the malignant transformation of epithelial cells requires further investigation.

Among immune cells, monocytes are the major source of IL-19 [21]. One study [20] reported that neither resting nor stimulated T cell or natural killer (NK) cells expressed IL-19, and another study [21] reported that healthy and Epstein Barr virus-transformed human B cells expressed IL-19 only in small amounts. In the present study, we found that B cell lymphoma was stained positive for

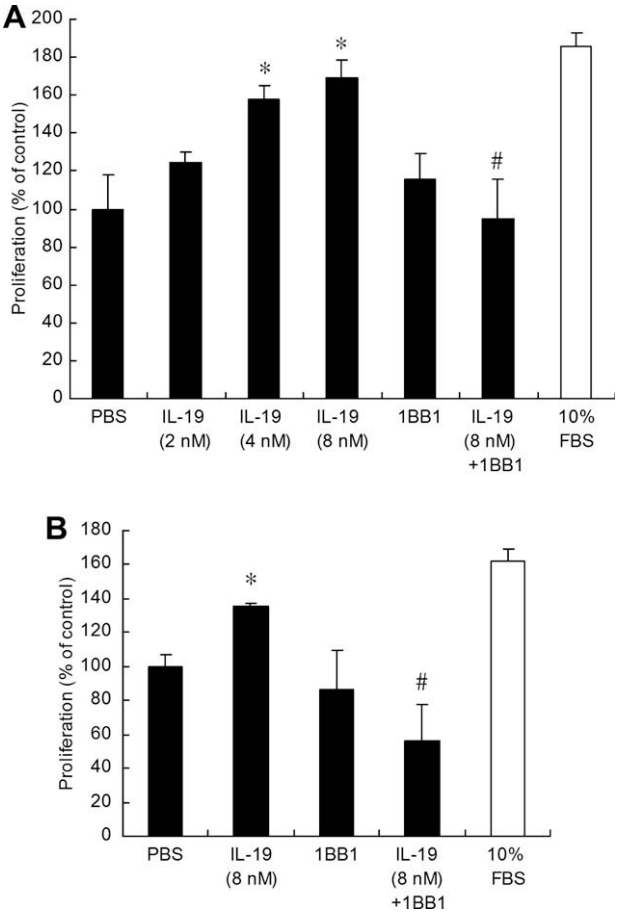

Fig. 7. IL-19 induced proliferation of oral cancer cell lines. OEC-M1 (A) and OC3 (B) cells were treated with various concentration of IL-19 for 48 h. The proliferation of OEC-M1 and OC3 cells were determined by MTT assay ($^*P < 0.05$ versus control). Anti-IL-19 monoclonal antibodies (1BB1, 20 nM) was used to specifically neutralize the proliferative activity of IL-19 ($^\#P < 0.05$ versus IL-19 (8 nM)). Fetal bovine serum (FBS) was used as a positive control. Values are means ± SEM of triplicate experiments.

IL-19, suggesting that IL-19 may be involved in B cell-lineage neoplasm.

We recently [10] confirmed that IL-19 induced apoptosis and chemoattractant production in a lung carcinoma cell line, and that it also induced neutrophil chemotaxis *in vitro*, which indicated that IL-19 is a chemoattractive factor. The present study showed IL-19 activated intracellular AKT, a signal relating to tumor cell proliferation, in oral cancer cell lines, which indicated that IL-19 might act in an autocrine manner and be involved in tumor growth. We also showed that IL-19 induced proliferation of oral cancer cell lines. We therefore hypothesize that IL-19 is involved in tumor biology. It will be worthwhile to further explore its molecular mechanism.

Myoepithelial cells in prostate gland tissue stained positive for IL-19 is a distinctive finding. IL-19 may be useful as a myoepithelial marker. It also points to a potential clinical use for IL-19 in the evaluation of prostate biopsies: the presence or absence of myoepithelial cells may be one of the key elements in distinguishing benign from malignant glands. Markers such as cytokeratin 34 β-E12 and p63 are currently used to highlight myoepithelial cells in the prostate [28]. It may be worthwhile to examine whether IL-19 adds additional value to the test.

In summary, this is the first study to use a tissue microarray and immunohistochemical staining to investigate the distribution, by tissue type and specific cell type, of IL-19 expression. Epithelial cells, endothelial cells, and macrophages were the major cell types stained positive for IL-19. We also found several types of tumor cells that were positively stained for IL-19, especially SCC cells, which were widely distributed in several types of tumor tissue. We also showed that IL-19 acted on SCC in an autocrine manner. Our data will provide valuable references for further investigation of the biological functions and clinical implications of IL-19 in humans.

Acknowledgments

We thank Mr. Tun-Yi Mou, Department of Physics, National Cheng Kung University, for building our arrayer. We also thank the Center of Excellence for Clinical Trial and Research in Oncology Specialty (supported by grant DOH-TD-B-111-004 from Department of Health, Taiwan) for providing the tissue arrayer service.

References

[1] Conti P, Kempuraj D, Frydas S, Kandere K, Boucher W, Letourneau R, et al. IL-10 subfamily members: IL-19, IL-20, IL-22, IL-24 and IL-26. Immunol Lett 2003;88:171–4.
[2] Fickenscher H, Hor S, Kupers H, Knappe A, Wittmann S, Sticht H. The interleukin-10 family of cytokines. Trends Immunol 2002;23:89–96.
[3] Pestka S, Krause CD, Sarkar D, Walter MR, Shi Y, Fisher PB. Interleukin-10 and related cytokines and receptors. Annu Rev Immunol 2004;22:929–79.
[4] Langer JA, Cutrone EC, Kotenko S. The class II cytokine receptor (CRF2) family: overview and patterns of receptor-ligand interactions. Cytokine Growth Factor Rev 2004;15:33–48.
[5] Kotenko SV. The family of IL-10-related cytokines and their receptors: related, but to what extent? Cytokine Growth Factor Rev 2002;13:223–40.
[6] Gallagher, Dickensheets H, Eskdale J, Izotova LS, Mirochnitchenko OV, Peat JD, et al. Cloning, expression and initial characterization of interleukin-19 (IL-19), a novel homologue of human interleukin-10 (IL-10). Genes Immun 2000;1:442–50.
[7] Hsing CH, Hsieh MY, Chen WY, Cheung So E, Cheng BC, Chang MS. Induction of interleukin-19 and interleukin-22 after cardiac surgery with cardiopulmonary bypass. Ann Thorac Surg 2006;81:2196–201.
[8] Liao YC, Liang WG, Chen FW, Hsu JH, Yang JJ, Chang MS. IL-19 induces production of IL-6 and TNF-alpha and results in cell apoptosis through TNF-alpha. J Immunol 2002;169:4288–97.
[9] Liao SC, Cheng YC, Wang YC, Wang CW, Yang SM, Yu CK, et al. IL-19 induced Th2 cytokines and was up-regulated in asthma patients. J Immunol 2004;173:6712–8.
[10] Hsing CH, Chiu CJ, Chang LY, Hsu CC, Chang MS. Il-19 is involved in the pathogenesis of endotoxic shock. Shock 2008;29:7–15.
[11] Gallagher G, Eskdale J, Jordan W, Peat J, Campbell J, Boniotto M, et al. Human interleukin-19 and its receptor: a potential role in the induction of Th2 responses. Int Immunopharmacol 2004;4:615–26.
[12] Hsing CH, Hsu CC, Chen WY, Chang LY, Hwang JC, Chang MS. Expression of IL-19 correlates with Th2 cytokines in uraemic patients. Nephrol Dial Transplant 2007;22:2230–8.
[13] Li HH, Lin YC, Chen PJ, Hsiao CH, Lee JY, Chen WC, et al. Interleukin-19 upregulates keratinocyte growth factor and is associated with psoriasis. Br J Dermatol 2005;153:591–5.
[14] Kononen J, Bubendorf L, Kallioniemi A, Barlund M, Schraml P, Leighton S, et al. Tissue microarrays for high-throughput molecular profiling of tumor specimens. Nat Med 1998;4:844–7.
[15] Bubendorf L, Nocito A, Moch H, Sauter G. Tissue microarray (TMA) technology: miniaturized pathology archives for high-throughput in situ studies. J Pathol 2001;195:72–9.
[16] Schraml P, Kononen J, Bubendorf L, Moch H, Bissig H, Nocito A, et al. Tissue microarrays for gene amplification surveys in many different tumor types. Clin Cancer Res 1999;5:1966–75.
[17] Kallioniemi OP, Wagner U, Kononen J, Sauter G. Tissue microarray technology for high-throughput molecular profiling of cancer. Hum Mol Genet 2001;10:657–62.
[18] Goding JW. Monoclonal antibodies: principles and practice. London: Academic Press; 1983.
[19] Yang SC, Lin SC, Chiang WF, Yen CY, Lin CH, Liu SY. Areca nut extract treatment elicits the fibroblastoid morphological changes, actin reorganization and signaling activation in oral keratinocytes. J Oral Pathol Med 2003;32:600–5.
[20] Lin SC, Liu CJ, Chiu CP, Chang SM, Lu SY, Chen YJ. Establishment of OC3 oral carcinoma cell line and identification of NF-kappa B activation responses to areca nut extract. J Oral Pathol Med 2004;33:79–86.
[21] Wolk K, Kunz S, Asadullah K, Sabat R. Cutting edge: immune cells as sources and targets of the IL-10 family members? J Immunol 2002;168:5397–402.
[22] Kunz S, Wolk K, Witte E, Witte K, Doecke WD, Volk HD, et al. Interleukin (IL)-19, IL-20 and IL-24 are produced by and act on keratinocytes and are distinct from classical ILs. Exp Dermatol 2006;15:991–1004.
[23] Zhong H, Wu Y, Belardinelli L, Zeng D. A2B adenosine receptors induce IL-19 from bronchial epithelial cells, resulting in TNF-alpha increase. Am J Respir Cell Mol Biol 2006;35:587–92.
[24] Jordan WJ, Eskdale J, Boniotto M, Lennon GP, Peat J, Campbell JD, et al. Human IL-19 regulates immunity through auto-induction of IL-19 and production of IL-10. Eur J Immunol 2005;35:1576–82.
[25] Hsing CH, Ho CL, Chang LY, Lee YL, Chuang SS, Chang MS. Tissue microarray analysis of interleukin-20 expression. Cytokine 2006;35:44–52.
[26] Wei CC, Chen WY, Wang YC, Chen PJ, Lee JY, Wong TW, et al. Detection of IL-20 and its receptors on psoriatic skin. Clin Immunol 2005;117:65–72.
[27] Nagalakshmi ML, Murphy E, McClanahan T, de Waal Malefyt R. Expression patterns of IL-10 ligand and receptor gene families provide leads for biological characterization. Int Immunopharmacol 2004;4:577–92.
[28] Sheikh F, Baurin VV, Lewis-Antes A, Shah NK, Smirnov SV, Anantha S, et al. Cutting edge: IL-26 signals through a novel receptor complex composed of IL-20 receptor 1 and IL-10 receptor 2. J Immunol 2004;172:2006–10.